# Analysis of Experimental Results on Electrical Wire Explosion in Water Taking into Account the Equivalent Generator Circuit[1]

A.G. Rousskikh, R.B. Baksht, S.A. Chaikovsky, A.Yu. Labetsky, V.I. Oreshkin, A.V. Shishlov

*High Current Electronics Institute, Akademichesky Ave., 4, Tomsk, Russia, Phone (3822) 492133, Fax(3822) 491677, E-mail: russ@ovpe2.hcei.tsc.ru*

**Abstract – Experimental values of exploding tungsten wire resistivity in water as a function of deposited energy under different power of input energy are given. These resistivity functions were obtained by a mathematical data conversion of the experimental current and voltage oscillograms taking into account the equivalent generator circuit. It was shown that the designed equivalent generator circuit describes adequately both the amplitude-frequency response and the transient oscillations. The design procedure of the equivalent generator circuit and its calibration in the regimes of short circuit, idle running and resistor load is given. The calculation metering error of deposited energy and the exploding wire resistivity were estimated for the case when calculation was carried out without taking into consideration the load inductive impedance.**

## 1. Introduction

Although a lot of research works concerning both the microsecond and nanosecond wire electrical explosions have been carried out, an interest in such investigations, which is determined both by the fundamental character of the phenomenon and its possible applications, still remains. One of such applications is imploding tungsten wire arrays used as a high power source of soft X-ray radiation [1–6]. Wire array optimization is associated with simulation both of the wire array implosion process and the electrical explosion of a separate wire. MHD modeling of the wire electrical explosion is performed taking into account the tungsten wire conductivity value that in its turn is a function of wire density and temperature. To check the simulation correctness, the calculation results should be compared with the experimental data, i.e. the calculated current and voltage values should be compared with the experimental current and voltage oscillograms. For this comparison, one needs a equivalent generator circuit. Simulating a wire explosion with a current rise time about or more than one microsecond we can neglect such circuit elements as stray capacitance, distributed inductance and the transient switch response [7]. However, the wire array explosion time is less than 100 ns and therefore, it is very important to have a detailed equivalent circuit. The equivalent generator circuit used earlier [8] was able to properly describe the oscillation period, the peak amplitude, the attenuation constant in the short circuit regime but was not able to properly describe the voltage inductive load oscillations in the short circuit regime, the voltage A-K gap oscillations in the idle running regime, the current and voltage leading edge shapes.

Thus, an object of these work was: 1) to obtian wire resistivity as a function of deposited energy under different parameters both of the generator circuit and the wire taking into account the equivalent generator circuit; 2) to create an adequate equivalent circuit of the current generator including a measurement circuit; 3) to estimate a metering error of the wire resistivity determination in the case the generator and the measurements circuit parameter are not taken into account.

## 2. Experimental Setup

To investigate the wire explosion process a *RLC*-generator was used. The equivalent generator circuit of is shown in Fig. 1. The wire explosion was carried out in deionized water with a resistivity greater than 150 kΩ·cm. The tungsten wires had diameters equal to 6.35, 15.24, and 30.48 μm. The wire length was 20 ± 0.5 mm.

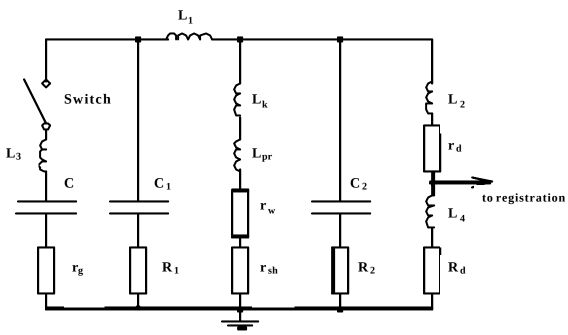


Fig. 1. Equivalent circuit of current generator: $r_g$, $r_{sh}$, $r_w$, $r_d$, $R_d$ – resistance of generator, shunt, wire, low resistance arm of divider circuit, high resistance arm of divider circuit; $R_1$, $R_2$ – distributed resistance; C – generator capacitance; $C_1$, $C_2$ – distributed capacitance; $L_1$ – circuit inductance; $L_2$, $L_4$ – divider inductance; $L_k$ – holder inductance; $L_{pr}$ – wire inductance

[1] The work was supported by ISTC project No. 1826.

The charge voltage was $U_0$ = 10, 22, and 30 kV. The circuit inductance was 740, 2100, and 11100 nH (without wire inductance $L_{pr}$). The capacitance was 67.9 nF. The switch was an air trigger. Five shots were made in each regime. A wire was fixed in a special holder (Fig. 2). To prevent sparking, the contact point between the electrodes and the wire was soldered and then cleaned with water and spirit. A high voltage divider, a coaxial shunt and a B-dot loop were used for electrical diagnostics.

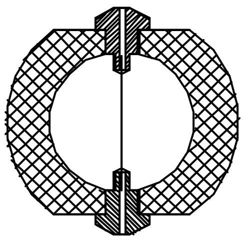

Fig. 2. Holder with a wire

## 3. Equivalent Generator Circuit Construction and its Calibration

The equivalent circuit of a current generator (see Fig. 1) was constructed on basis of a careful model analysis. Determination of separate circuit parameters was carried out from the comparison of the experimental current and the voltage oscillograms with the results of the numerical solution of circuit differential equations in the regimes of short circuit, idle running and resistor load (see Fig. 3,*a*–*c*). Using of two additional *RLC* circuits allowed us to describe the circuit oscillations that are observed in the idle running regime (see Fig. 3,*a*).

To adequately describe the voltage and current front shapes (see Fig. 3,a) we had to reject an ideal switch and describe real trigger parameters as a function model [9]:

$$r_{kl} = \frac{A}{\left[\left(\int |I| \cdot dt\right)^{B} + C\right]}, \qquad (1)$$

where $r_{kl}$ is the trigger resistance, $I$ is the current through the trigger, $t$ is the time in ns, À = 27500, Â = 0.83, Ñ = 2000.

The oscillograms in the short circuit regime (see Fig. 3,*c*) were registered with several different load inductance. For that purpose, the holder with the wire (see Fig. 2) was replaced by a cylinder with the diameters 1.2, 3, 10, 24 and 98 mm. Considerations of all measurements allows finding out the value of the load inductance $L_n$. That value is necessary for taking into account the inductive component of the measured voltage. The value of inductance $L_n$ was calculated on the assumption of formula (2) [10] that defines the value of the wire inductance $L_{pr}$:

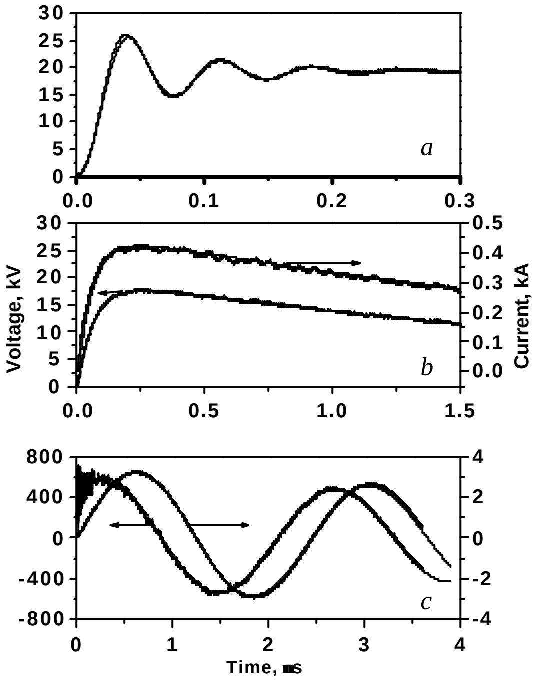


Fig. 3. Comparison of experimental oscillograms in regimes of *a* – idle running, *b* – resistor load (42 Ω) and *c* – short circuit with results of numerical solution of circuit differential equations

$$L_{pr} = \frac{\mu_0}{2\cdot\pi}\left[\ln\left(\frac{R}{p}\right) + \frac{1}{m}\ln\left(\frac{R}{m\cdot\rho}\right) + \frac{1+m}{4\cdot m}\right], \qquad (2)$$

where $R$ is the radius of current return posts, $p$ is the wire radius, $\rho$ is the post radius, $m$ is the number of posts.

## 4. Metering Error Estimation

Measurements of voltage applied to a load is the point of maximal error in the determination of the energy deposited in the wire and its resistivity. The calculation procedure described in [11] does not take into account either the distributed character of capacitance or the energy consumption in a switch, therefore it cannot be free from some mistakes. To estimate the calculation metering error of the deposited energy and the exploding wire resistivity for the case when the calculation was carried out without taking into consideration the load inductive impedance, the folliwing procedure was used. The wire resistivity was simulated with the interpolation formula of functional dependence of the 30-μm tungsten wire resistivity on the deposited energy that was obtained in the experiment (reference resistivity). The voltage applied to the high voltage divider (divider voltage), the voltage applied to wire and the load current were calculated solving a system of circuit differential equations. Using the simulated value of the divider voltage and the load current, the functional dependence of the wire resistivity on the deposited energy was calculated anew but without taking into account the load inductive impedance. The resulting curve was compared with the reference resistivity. Based on that comparison the error estimations of the deposited energy without taking into account the inductive impedance of a wire load were made. One of these estimations is shown in Fig. 4.

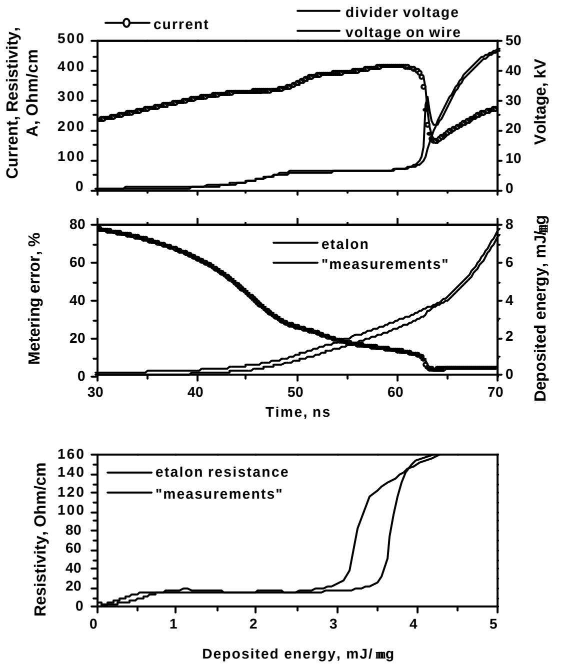


Fig. 4. Estimation of metering error of measurements

### 5. Experimental Results

The resistivity of the tungsten wires whose diameters were 6.35, 15.24, 30.48 μm as a function of the specific deposited energy is given in Fig. 5,*a–c*, Fig. 6,*a–c* and Fig. 7,*a–c*, respectively. As follows from Figs. 5–7, the energy deposited in the wire increases with increasing generator power. Under a regime where the charge voltage $U_0$ was equal to 10 kV or 20 kV, hydrodynamical instability development has a great influence on the deposited energy value and leads to wire destruction before the moment of the wire total sublimation ($E_{subl}$ = 5.69 mJ/μg). The comparison of the experimental wire resistivity as a function of the deposited energy with the known tabular data [12, 13] is given in Fig. 8. As follows from Fig. 8, the tabular data coincide with the experimental ones except for the energy values range close to the melting zone.

It necessary to mention that the electrical explosion of the 6.35 μm-diameter wire is accompanied by high amplitude reproducible fluctuations of the wire resistivity. Probably, a reason for the arising fluctuations can be related to appearance of the capillar waves [14] which wavelength is about 1 μm on the melted wire surface. The capillar waves wavelength is comparable with the fine wire diameter and able to generate a fluctuations of the wire resistivity. It is possible to assume that the rapidly fluctuating wire resistance combined with the distributed generator circuit parameters gives rise to the fluctuation of the load voltage. However, that question needs further research.

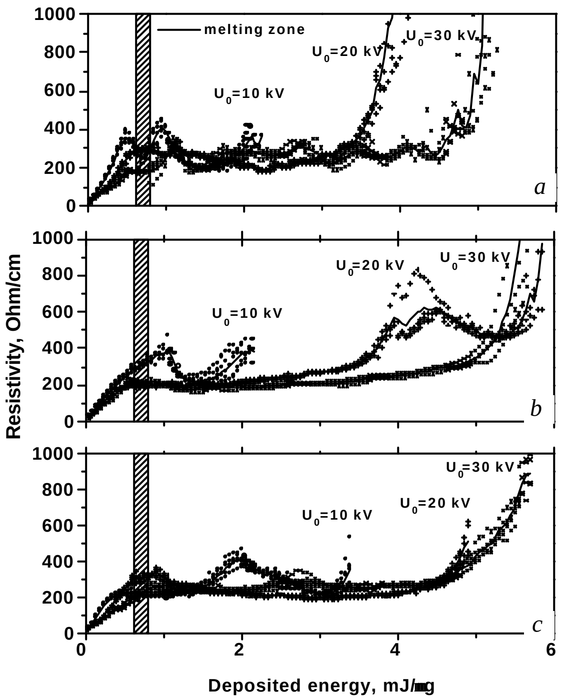


Fig. 5. The specific resistance of tungsten wires with diameters 6.35 μm under: $L_1$ = 635 nH (*a*); $L_1$ = 2000 nH (*b*); $L_1$ = 11100 nH (*c*). Solid line is average value of experimental data

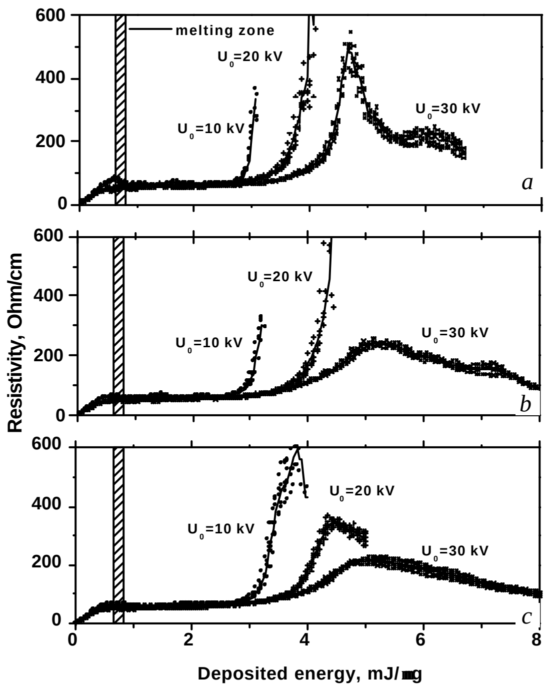


Fig. 6. The specific resistance of tungsten wires with diameters 15.24 μm under: $L_1$ = 635 nH (*a*); $L_1$ = 2000 nH (*b*); $L_1$ = 11100 nH (*c*). Solid line is an average value of experimental data

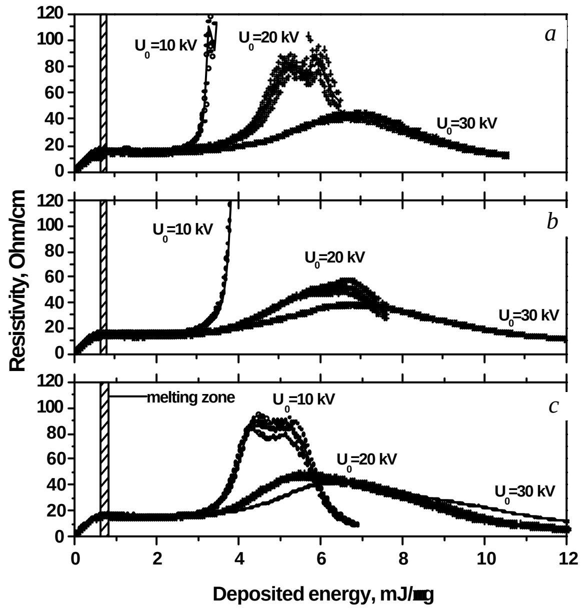


Fig. 7. The specific resistance of tungsten wires with diameters 30.24 µm under: $L_1$ = 635 nH (*a*); $L_1$ = 2000 nH (*b*); $L_1$ = 11100 nH (*c*). Solid line is average value of experimental data

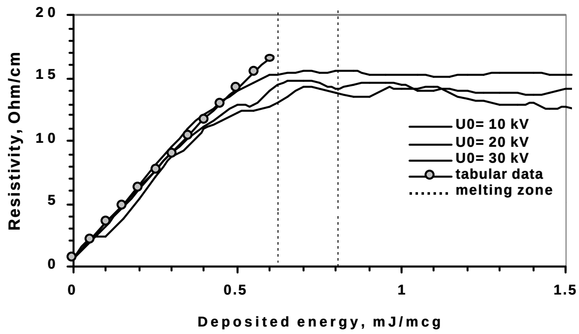


Fig. 8. The comparison of the experimental wire resistivity with the tabular data. $L_1$ = 2000 nH, the wire diameter is 30 µm

## 6. Conclusion

The conducted experiments have allowed us to get the tungsten wire resistivity in depending on the deposited energy under different values of the deposited energy power. The findings and the existence of the detailed equivalent circuit of the current generator make it possible to compare in detail the simulated and experimental results. The circuit analysis shows that the deposited energy calculation without taking into account the load inductive impedance leads to a metering error of 10÷15%. The metering error of time response of the deposited energy in that case can achieve 100% (at the beginning of explosion). The time response calculation of the wire resistivity as a function of deposited energy without taking into account the inductive load impedance leads to a metering error exceeding 100% (in the range of small values). Using a detailed equivalent generator circuit it is possible to decrease the metering error of the determination of the wire resistivity to about 3%, that is less than the measurement jitter.

## References

[1] R.B. Spielman, C. Deeney, G.A. Chandler et al., Phys. of Plasmas **5**, 2105 (1998).

[2] J.P. Apruzese, P.E. Pulsifer, J. Davis et al., Phys. of Plasmas **5,** 4476 (1998).

[3] C. Deeney, C.A. Coverdale, M.R. Douglas et al., Phys. of Plasmas **6,** 2081 (1999).

[4] I.H. Mitchell, J.M. Bayley, J.P. Chittenden, J.F. Worley, A.E. Dangar, and M.G. Haines, Rev. Sci. Instrum. **67**, 1533 (1996).

[5] V.V. Alexandrov, I.N. Frolov, M.V. Fedulov, E.V. Grabovsky et al., IEEE Transaction on Plasma Science **30/2**, 559 (2002).

[6] T.A. Shelkovenko, S.A. Pikuz, D.B. Sinars, K.M. Chandler, and D.A. Hammer, Physics of Plasmas **9/5**, 2165 (2002).

[7] V.S. Sedoi, G.A. Mesyats, V.I. Oreshkin et al., IEEE Trans. Plasma Sci. **27**, 845 (1999).

[8] A.G. Rousskikh, R.B. Baksht, V.I. Oreshkin, A.V. Shishlov, *in: Proc. 14$^{th}$ Int. Conf. on High-Power Particle Beams and 5$^{th}$ Int. Conf. on Dense Z-Pinches*, 2002, pp. 217–220.

[9] V.V. Kremnev, G.A. Mesyaz, *Pulse Multiplication and Transformation Methods in High Current Electronics*, Novosibirsk, Nauka, 1987, pp. 191–194.

[10] P.L. Kalantarov, L.A. Ceytlin, *Calculations of Inductance*, Leningrad, Energoatomizdat, 1986, p. 137.

[11] V.V. Bondarenko, I.F. Kvarzhava, A.A. Plutto, A.A. Chernov, Rus. J. of Exp. and Theor. Physics **28/2**, 191 (1955).

[12] A.V. Arutunuv, L.P. Filipov, *The thermal-physical characteristics of the pure substance,* edition 5, 1971.

[13] S.V. Koval, N.I. Kuskova, S.I. Tkachenko, High Temperature **6/35**, 876 (1997).

[14] L.D. Landau, E.M. Lifshits, *Hydrodynamics,* Moscow, Nauka, 1986, pp. 341–346.